Nature 526.7573 (2015): 380-384

DOI: https://doi.org/10.1038/nature14905

A Cretaceous eutriconodont and integument evolution of early mammals

Thomas Martin, Jesús Marugán-Lobón, Romain Vullo, Hugo Martín-Abad, Zhe-Xi Luo, Angela D. Buscalioni

Abstract We report a 125 Mya eutriconodontan mammal from Spain with extraordinary preservation of skin and pelage that extends the record of key mammalian integumentary features into the Mesozoic. The new mammalian specimen exhibits such typical mammalian features as pelage, mane, pinna, and a variety of skin structures: keratinous dermal scutes, hair-like tubules composing protospines, and compound follicles with primary and secondary hairs. The skin structures of this new Mesozoic mammal encompass the same combination of integumentary features as those evolved independently in other crown Mammalia, with similarly broad structural variations as in extant mammals. Soft tissues in the thorax and abdomen (alveolar lungs and liver) suggest the presence of a muscular diaphragm. The eutriconodont has molariform tooth replacement, ossified Meckel's cartilage of the middle ear, and specialized xenarthrous articulations of posterior dorsal vertebrae, convergent with extant xenarthran mammals, that strengthened the vertebral column in locomotion.

Mammals have diverse integumentary structures such as hair, spines and scutes[1]. Fossilized fur is known for Mesozoic mammals from the Middle Jurassic onwards, and can be traced back to the early-divergent mammaliaform clades[2-7]. So far, however, fur has fossilized only as hair impressions and compressions, types of preservation that rarely show microstructure. The exceptional phosphatized preservation of skin tissues in the specimen from Las Hoyas extends direct knowledge of mammalian integumentary microstructure from 60 Mya (late Paleocene)[8] back to 125-127 Mya (Early Cretaceous). The new Spanish gobiconodontid (Eutriconodonta, Mammalia) combines a complete and articulated skeleton, with extraordinary preservation of skin, hair, keratinous dermal scutes, and remnants of visceral organs.

The most striking feature of extant mammalian hairs is their outstanding polymorphism[9], among closely related species, at different developmental stages, and even in the same individual. The new fossil shows the prominent polymorphism in a variety of keratinous appendages, some of which are described for Mesozoic mammals for the first time. The cylindrical structures (protospines) are formed from the fusion of micro-cylindrical tubules, architecturally similar to the spines of modern mammals. Such protospines represent the earliest record of a microstructure analogous to that of spiny mice (*Acomys*) and hedgehogs (*Erinaceus*). As in extant mammals, hair shafts have three architectural units: cortex, medulla, and cuticles with varied designs. Moreover, at a microscopic scale the epidermal layer preserves compound follicles with more than two hairs stemming from the same follicle. The structural diversity of hairs in this new mammaliaform indicates that polymorphism of hairs and related structures is likely correlated with the same developmental process as in extant mammals[9].

On its posterior dorsal vertebrae the new eutriconodont has additional xenarthrous articulations in addition to the usual zygapophyses. This is well known for Xenarthra (armadillos, anteaters, and sloths) among extant placentals and similar structures have been observed in some Eocene eutherians[10-12]. The fact that features of xenarthral articulation are also present in the Late Jurassic mammaliaform *Fruitafossor*[13], makes the new mammal from Spain another case of convergent evolution of this remarkable skeletal feature that strengthens the dorsal vertebral column for versatile locomotor functions.

Class Mammalia[14]

Order Eutriconodonta[15]

Family Gobiconodontidae[16]

Spinolestes xenarthrosus gen. et sp. nov.

Etymology. Spinosus (Latin), in reference to the spiny integument; λέστης (Greek) or lestes (Latin spelling), meaning robber and a common term in taxonomic name of mammals. The specific name *xenarthrosus* refers to the special additional (ξένος, [Greek] strange) articulation facets (ἄρθρον, [Greek] articulation) of the dorsal vertebrae.

Holotype. MCCMLH30000, Museo de las Ciencias de Castilla-La Mancha. A complete skeleton with integumentary structures preserved. Skeletal and integumentary remains of the slab MCCMLH30000A were transferred to a matrix of epoxy resin in preparation, to expose the embedded side of the fossil, but are kept intact in the counter slab MCCMLH30000B (Figs. 1, 4a, Ext. Data Fig. 1). Life Science Identifier (LSID): urn:lsid:zoobank.org:act:10B31072-A727-4663-A7DC-4224FB97E1E3.

Locality and horizon. La Hoyas Quarry, Calizas de la Huérgina Formation, southwestern Iberian Basin (Cuenca, Spain). Las Hoyas is latest Barremian (125-127 Mya) in age, based on charophytes and ostracodes[17]. The Las Hoyas Konservat-Lagerstätte occurs in finely laminated limestones deriving from a freshwater wetland. Fossils are usually preserved fully articulated including soft tissues such as mineralized muscle and skin. Potential mechanisms for exquisite preservation are microbial mats, anoxia, and rapid burial by sediments[18].

Diagnosis. Dental formula I^3-C^1-P^2-M^4/i_3-c_1-p_2-m_4. Cheek teeth of general "amphilestid" pattern (Fig. 2a-d). Differs from stem mammaliaforms in lacking the postdentary trough. Differs from the "amphilestids" *Amphilestes* and *Phascolotherium* in fewer premolars, fewer molariforms, or both; from *Hakusanodon*[19] and *Juchilestes*[20] in fewer molariforms. Differs from *Jeholodens* and *Yanoconodon*[21, 22] by the presence of accessory cusps d and e of lower molariforms and a lingual cingulum in upper molariforms. Differs from *Liaoconodon*[23] in having one fewer lower incisor and one more upper molariform, and lacking the uniform enlargement of incisors and canines of the latter. Differs from genera of the Triconodontidae in absence of vertical tongue-in-groove interlock of molariforms, and more uniform heights of cusps of the latter. Unique among gobiconodontids in that the erupting (replacing) molariform is lingual (side-by-side) to the deciduous molariform of the same tooth locus (Video S1). Within gobiconodontids, *Spinolestes* differs from *Gobiconodon*[24-26] in having more incisors and fewer premolars. Of all gobiconodontids, *Spinolestes* is most similar to *Repenomamus* in dentition, but differs from *Repenomamus* species in having one fewer molariform each for uppers and for lowers, in enlargement of lower first incisor, and in having both labial and lingual cingula at upper molariforms[27] (for full diagnosis and phylogenetic hypothesis see Fig. 3 and Supplementary Information).

Description

The skeleton is exposed on its right lateral side in the main slab after its transfer to resin embedding. The skull is exposed on its ventral side (Figs. 1b, 4a, Ext. Data Fig. 1) and has a rounded rostrum. The jugals are complete, extending from anterior zygoma to the squamosal glenoid. The glenoid is transversely expanded. The petrosal has a cylindrical promontorium, and a narrow lateral trough. The occipital condyles are large and oval shaped. The mandibles are robust for their short length, and have no angular process. The dentary condyles are broadly oval and bent laterally from the plane of coronoid process and mandibular body. Meckel´s cartilage is ossified, preserved in situ on the left mandible but detached on the right side, exposing a wide Meckel's groove on the right mandible (Video S2). The middle ear bones themselves are lost, but given the curved Meckel's cartilage, we infer the ear was medio-laterally separate from the mandible yet still connected antero-posteriorly to the mandible via the ossified Meckel's cartilage, as in *Yanoconodon*, *Liaoconodon*, and other gobiconodontids[22, 23, 25, 28].

Spinolestes shows lower molariform replacements at least at m1 to m2 loci (Fig. 2a, b). The right m1 and m3 are in the process of eruption whereas beneath deciduous m2 the germ of replacing m2 is visible. Upper molariform replacements occur from M1 to M4 positions. The right M1 is in the process of eruption. Deciduous M3 and M4 are heavily worn in an oblique angle, down to the roots, but still in place in the maxilla, while replacing M3 and M4 are erupting to the lingual side of DM3, DM4 although at different stages (Video S1). Medial molariform replacement/succession occurs only in the maxilla, but mandible shows vertical replacement of deciduous by erupting molariforms. Because upper M2 appears to have erupted earlier than M1 and M3, and lower m1 and m3 erupted before m2, *Spinolestes* shows alternative replacements for these tooth loci. Alternating replacement is common in basal mammals[29], and is consistent with replacement patterns of anterior molariforms in *Gobiconodon ostromi*[24].

The shoulder girdle is therian-like (Fig. 1a, b). The broad, triangular scapula has a high spine that ends in a cranially oriented acromion. Its posterior border is laterally bent, forming a secondary spine. As in therians, the glenoid fossa is oval, oriented nearly perpendicular to the scapular plate. The curved clavicle has a large, curved synovial facet on its distal end for mobile articulation with the acromion. The coracoid is small and fused to the scapula. There is no procoracoid. Five ossified sternal elements are present, plus the partially preserved interclavicle in the ventral part of the thorax. The claviculo-interclavicular joint is mobile, as documented for other eutriconodonts[21, 22, 27].

Spinolestes has 16 thoracic vertebrae, seven lumbar vertebrae (defined by zygapophyses rotated to vertical, and by transverse processes), three fused sacrals, and 22 caudals. 20 dorsal vertebrae bear ribs, of which 16 pairs are associated with the thoracic and four pairs with the lumbar vertebrae. Ultimate and penultimate lumbars have fused ribs. The robust ribs are two-headed, and have rounded cross sections. The dorsal vertebrae have reclined spinal processes. Beginning with dorsal vertebra 11, the spinal processes become larger in the antero-posterior dimension, and develop an expanded flat-top. This flat-top becomes larger and more prominent in the successively more posterior lumbars.

Spinolestes shows accessory lateral xenarthrous articulations (sensu ref. 30) from dorsal vertebrae 9/10 through dorsals 17/18 (Fig. 2e-g). The anterolateral aspect of the prezygapophysis forms a lateral zygapophyseal articulation with the preceding vertebra. Among therian mammal groups, xenarthrous articulation is most prominently developed in South American xenarthrans (armadillos, anteaters, and sloths), and in some Eocene placentals[10-12]. Among Mesozoic mammaliaforms, a xenarthrous articulation is present in *Fruitafossor*[13]. Besides *Spinolestes*, this derived structure is also present in other gobiconodontids according to our observation (also ref. 27: figs. 3-8, 3-10). However, gobiconodontids including *Spinolestes*, and the mammaliaform *Fruitafossor* lack the fully developed mammillary process (metapophysis[31]) of the xenarthrous articulation seen in xenarthran placentals.

Phylogenetic relationships and palaeobiogeography

Two phylogenetic analyses were conducted (Fig. 3). One estimates the relationships of *Spinolestes* among major mammaliaform clades (Fig. 3b on a dataset of 111 taxa and 490 characters[7, 28]), and the other evaluates the placement of *Spinolestes* among 20 genera of eutriconodonts (Fig. 3a, based on 90 dental and mandibular characters[19, 20, 32, 33]). *Spinolestes* is nested within Eutriconodonta as a member of Gobiconodontidae. Within Gobiconodontidae, *Spinolestes* is the sister-taxon of the clade *Gobiconodon* + *Repenomamus*. The finer sampling of eutriconodont taxa improves the resolution of the known eutriconodont phylogenies[29, 32, 33]. In fact, gobiconodontids have a broad distribution from Asia to North America during the Early Cretaceous (Barremian to Albian), and are relatively abundant in Asia. The discovery of *Spinolestes*, plus two gobiconodontid teeth from the Early Cretaceous of Spain[34] and Britain[35] has extended the distribution of this family to Western Europe. This is consistent with the broad interchanges of other mammal groups on the Laurasian landmass during the Early Cretaceous[29].

Integumentary and soft-tissue structures

The *Spinolestes* specimen shows regional hair differentiation and exquisite preservation of many integumentary structures (Fig. 4, Ext. Data Figs. 1-7). A dense mane of long guard hairs (3-5 mm long) (Fig. 4b) is developed in the parietal, cervical, and scapular regions. Long and fine hairs are also present along the dorsal region, where they form a median crest, and along most of the tail. The rest of the body is covered by a soft and dense underfur (Fig. 4j).

Multiple pieces of skin are preserved with microstructural details of hair such as primary and gradually smaller secondary hairs that are organized in compound follicles (Fig. 4c, d, i, Ext. Data Figs. 2-4), as in many modern placentals[36-38], marsupials, and monotremes[39]. In an isolated piece of skin between dorsal vertebrae 11 and 14, compound follicles are associated with scale-like folds of the skin (Ext. Data Fig. 2c), identical to the pattern of hairy skin of extant dogs[36] (Ext. Data Fig. 2d). The cuticular scales have a smooth surface. The cuticula of primary hairs shows an irregular mosaic of imbricate, ovate scales (Fig. 4 i, Ext. Data. Fig. 3a-c). The cuticula of secondary hairs displays coronal scales (annulus and encircling the shaft) with either simple or serrate free margins (Fig. 4i, Ext. Data Fig. 3b, c). The longitudinal section of a primary hair shaft exhibits a discontinuous medulla with serial chambers and septa, and a thick cortex made of typical fusiform, spindle-shaped cells (ref. 40: fig. 3) (Fig. 4 g, Ext. Data Fig. 5). In a few regions of the body the hairs have short, truncated shafts less than 1 mm long (Fig. 4c, d) with dark-colored distal ends. Compared with normal hairs, such features match the so-called “block hairs” and “i-hairs” that represent a pathological condition associated with a fungal infection (dermatophytosis) widely spread in extant mammals (ref. 41: fig. 2.50).

Spinolestes has what we call here protospines in the dorso-sacral region of the body (Fig. 4 e, f), varying in basal diameters from 80 to 130 µm. Each of these small protospines is made up of two or more longitudinally fused tubules that appear to have scaly external surface, and an interior medullary cavity surrounded by a cortical structure (Fig. 4f). These tubules are interpreted as modified primary and secondary hairs. Most of the thicker protospines cluster with thinner ones and with isolated tubules, all of which are oriented randomly. A dozen or so oval dermal scutes up to 4 mm in dimension are present in the dorsal, lumbar and pelvic regions (Fig. 4 h, Ext. Data Fig. 7). These scutes consist of a random arrangement of tubules merging to a homogeneous matrix.

Spines and hairs have fundamentally similar structural designs[9, 42]. In embryogenesis, spines appear later than hairs and are developed from the fusion of several hair follicles either by the merger of multiple hair follicles of similar size, or by one large merging with several and smaller surrounding hair follicles[9]. SEM revealed that the protospines of *Spinolestes* are formed by merger of several hair-

like tubules, which is similar to the development of spines from the fusion of hair follicles in extant mammals. The co-existence of compound hair follicles by which primary and secondary hairs are bundled, and the clustering of spines and tubules in *Spinolestes*, provides fossil evidence on an early stage of spine evolution in mammals. This suggests that the evolution of spines was mediated in Mesozoic mammals by a similar process of fusion of multiple hair follicles, as in the embryogenesis of integumentary structures in extant mammals. The unambiguous presence of compound hair follicles and their related scale-like skin folds in such a basal mammal clade as eutriconodonts, confirm that these features are ancestral to mammals. *Spinolestes* further proves that mammalian underfur, guard hair, and spines had already fully differentiated in some Mesozoic mammals during the Early Cretaceous. The fact that multiple specimens of many taxa of eutriconodonts are preserved with fur but lack spines makes the presence of protospines in *Spinolestes* unique among eutriconodonts, apparently evolving independently from monotremes (echidnas), and some placentals such as hedgehogs and spiny mice. Although *Acomys* spines consist of a single modified awl hair, spiny mice can serve as modern analogue to *Spinolestes* with spiny hairs located on the lower dorsum, possibly for display and protection against predators by easy loss of spines when bitten into the back[43].

The specimen also shows a unique preservation of several organs. In the area of the scalp, the left outer ear (external pinna) is perfectly preserved (Fig. 4a, Ext. Data Fig. 6). Within the thoracic ribcage of *Spinolestes*, a patch of fossilized soft tissues contains tubular structures with a branching pattern (Ext. Data Fig. 8). From the position and distribution in the rib cage, this most likely represents fossilized lung tissue, and the branching structures likely represent the bronchioles of the lung[44]. Posteriorly to the lung tissue, a large oval area of reddish-brown soft-tissue (Ext. Data Fig. 8a) is interpreted as residues of the liver according to its anatomical position and color. Liver tissue is rich in iron, and provides a reddish color, as has been reported for the theropod *Scipionyx* from late Early Cretaceous (Albian) of Italy[45]. The boundary between the inferred lung and the liver tissues extends, obliquely, from the distal tip of the 3rd rib to the proximal end of the 15th rib (Ext. Data-Fig. 8a), corresponding to the muscular diaphragm in extant mammals[38]. This extends from the mid-sternal area to the posterior-most thoracic vertebrae, packed between the lungs, in the thorax, and the liver in the abdominal cavity. Its presence reconfirms that this complex respiratory apparatus, which is tightly correlated with locomotion[46], was already functional in Mesozoic mammals.

Skeletal and locomotor adaptations

The scaling of long bones to body mass[47, 48] estimates that the weight of *Spinolestes* ranged from 52 to 72 g (see biometrics in SI) indicating that it was a medium sized Mesozoic mammal, falling within

the range of small extant didelphid marsupials (e.g., the size of *Monodelphis brevicaudata* and *Marmosa murina*)[47]. Its limb proportions, and xenarthrous vertebrae configuration together encompass a singular ecomorphological combination. The fibula is not co-ossified with the tibia, and is only slightly thinner than the latter. The carpals are relatively short, and the value of phalangeal index[49] of digit III at 121 corresponding to the top quartile of mammals with a terrestrial locomotory mode, definitively indicates that it was not arboreal. The terminal phalanges lack a highly curved dorsal outline (Fig. 1 c), but are robust and relatively wide, both of which are features common for extant mammals of terrestrial and fossorial life styles. Many (although not all) extant placentals with xenarthrous vertebral articulations (or with reinforced thoracolumbar vertebrae in general) are capable diggers, such as armadillos and anteaters. The Jurassic mammaliaform *Fruitafossor* exhibits striking convergent adaptations to armadillos such as reduced enamel-less peglike teeth and xenarthrous vertebral articulations. The Eocene mammal *Eurotamandua* (putatively a palaeanodont) has edentulous jaws and strongly enlarged manual claws. Both taxa are considered as fossorial and feeding on colonial insects[10, 13]. In contrast to *Fruitafossor*, *Eurotamandua*, and xenarthrans, the dentition of *Spinolestes* does not exhibit any tendency to reduction. Thus, *Spinolestes* shows a mosaic of functional features, suggesting a terrestrial locomotion, with ambulatory gait, as in *Gobiconodon*[24, 27], and potential digging abilities, with a more versatile life style (Ext. Data Fig. 9). The extant armored shrew *Scutisorex* can serve as a modern analogue for the lifestyle of *Spinolestes*. S*cutisorex* is unique among mammals by its massive interlocking lumbar vertebrae which provide an extraordinary vertebral strength. It has been hypothesized that *Scutisorex* uses this vertebral strength to force open the base of palm leaves to search for insects or larvae in swampy forests[50]. A similar lifestyle, supported by the strong arms and hands, is hypothesized here for *Spinolestes,* which lived in the vegetated Las Hoyas wetland environment.

References

1. Alibardi, L. Perspectives on hair evolution based on some comparative studies on vertebrate cornification. *J. Exp. Zool.* 318B, 325-343 (2012).

2. Ji, Q. et al. The earliest known eutherian mammal. *Nature* 416, 816-822 (2002).

3. Ji, Q. et al. A swimming mammaliaform from the Middle Jurassic and ecomorphological diversification of early mammals. *Science* 311, 1123-1127 (2006).

4. Meng, Q.-J. et al. An arboreal docodont from the Jurassic and mammaliaform ecological diversification. *Science* 347, 764-768 (2015).

5. Meng, J. et al. A Mesozoic gliding mammal from northeastern China. *Nature* 444, 889-893 (2006).

6. Vullo, R. et al. Mammalian hairs in Early Cretaceous amber. *Naturwissenschaften* 97, 683-687 (2010).

7. Zhou, C.-F. et al. A Jurassic mammaliaform and the earliest mammalian evolutionary adaptations. *Nature* 500, 163-167 (2013).

8. Meng, J. & Wyss, A. R. Multituberculate and other mammal hair recovered from Palaeogene excreta. *Nature* 385, 712-714 (1997).

9. Chernova, O. F. Evolutionary aspects of hair polymorphism. *Biology Bull.* 33, 43-52 (2006).

10. Storch, G. *Eurotamandua joresi*, ein Myrmecophagide aus dem Eozän der "Grube Messel" bei Darmstadt (Mammalia, Xenarthra). *Senckenbergiana Lethaea* 61, 247-289 (1981).

11. Ting, S.-Y. A Paleocene edentate from Nanxiong Basin, Guangdong. *Palaeontol. Sinica*, New Series C 17, 85-118 (1987).

12. Rose, K. D. & Emry, R. J. in *Mammal Phylogeny: Placentals* (eds Szalay, F. S., Novacek, M. J. & McKenna, M. C.) 81-102 (Springer, New York, 1993).

13. Luo, Z.-X. & Wible, J. R. A Late Jurassic digging mammal and early mammalian diversification. *Science* 308, 103-107 (2005).

14. Linnaeus, C. *Systema naturae per regna tria naturae, secundum classes, ordines, genera, species, cum characteribus, differentiis, synonymis, locis.* Vol. 1. *Regnum animale*. Editio decima, reformata. 824 pp. Laurentius Salvius, Stockholm (1758).

15. Kermack, K. A. et al. The lower jaw *of Morganucodon*. *Zool. J. Linn. Soc-Lond.* 53, 87-175 (1973).

16. Chow, M. and Rich, T. H. V. A new triconodontan (Mammalia) from the Jurassic of China. *J. Vertebr. Paleontol.* 3, 226-231 (1984).

17. Fregenal-Martínez, M. A. & Meléndez, N. in *Lake Basins through Space and Time* (eds Gierlowski-Kordesch, E. H. & Kelts, K.) AAPG Studies in Geology 46, 303-314 (2000)

18. Buscalioni, A. D. & Fregenal-Martínez, M. A. A holistic approach to the palaeoecology of Las Hoyas Konservat-Lagerstätte (La Huérgina Formation, Lower Cretaceous, Iberian Ranges, Spain). *J. Iber. Geol.* 36, 297-326 (2010).

19. Rougier, G. W. et al. An Early Cretaceous mammal from the Kuwajima Formation (Tetori Group), Japan, and a reassessment of triconodont phylogeny. *Ann. Carnegie Mus.* 76, 73-115 (2007).

20. Gao, C.-L. et al. A new mammal skull from the Lower Cretaceous of China with implications for the evolution of obtuse-angled molars and 'amphilestid' eutriconodonts. *P. Roy. Soc. Lond. B Bio.* 277, 237-246 (2010).

21. Ji, Q. et al. A Chinese triconodont mammal and mosaic evolution of the mammalian skeleton. *Nature* 398, 326-330 (1999).

22. Luo, Z.-X. et al. A new eutriconodont mammal and evolutionary development in early mammals. *Nature* 446, 288-293 (2007).

23. Meng, J. et al. Transitional mammalian middle ear from a new Cretaceous Jehol eutriconodont. *Nature* 472, 181-185 (2011).

24. Jenkins, F. A. & Schaff, C. R. The Early Cretaceous mammal *Gobiconodon* (Mammalia, Triconodonta) from the Cloverly Formation in Montana. *J. Vertebr. Paleontol.* 8, 1-24 (1988).

25. Kielan-Jaworowska, Z. & Dashzeveg, D. Early Cretaceous amphilestid ("triconodont") mammal from Mongolia. *Acta Palaeontol. Pol.* 43, 413-438 (1998).

26. Li, C.-K. et al. A new species of *Gobiconodon* (Triconodonta, Mammalia) and its implication for the age of Jehol Biota. *Chinese Sci. Bull.* 48, 1129-1134 (2003).

27. Hu, Y.-M. *Postcranial morphology of* Repenomamus *(Eutriconodonta, Mammalia): Implications for the higher-level phylogeny of mammals.* Dissertation, City University of New York, 423 pp. (2006).

28. Luo, Z.-X. Developmental patterns in Mesozoic evolution of mammal ears. *Annu. Rev. Ecol. Syst.* 42, 355-380 (2011).

29. Kielan-Jaworowska, Z. et al. *Mammals from the Age of Dinosaurs. Origins, Evolution, and Structure*. 2004 (Columbia University Press, New York, NY).

30. Gaudin, T. J. The morphology of xenarthrous vertebrae (Mammalia: Xenarthra). *Fieldiana Geology*, n. s. 41, 1-38 (1999).

31. Lessertisseur, J. & Saban, R. in *Traité de Zoologi*e,Tome 16, Fascicule 1. Mammifères, Téguments et Squelette (ed Grassé, P. P.) 709-1078 (Masson et Cie, Paris, 1967).

32. Kusuhashi, N. et al. New triconodontids (Mammalia) from the Lower Cretaceous Shahai and Fuxin formations, northeastern China. *Geobios* 42, 765-781 (2009).

33. Gaetano, L. C. & Rougier, G. W. New materials of Argentoconodon fariasorum (Mammaliaformes, Triconodontidae) from the Jurassic of Argentina and its bearing on triconodont phylogeny. *J. Vertebr. Paleontol.* 31, 829-843 (2011).

34. Cuenca-Bescós, G. & Canudo, J. I. A new gobiconodontid mammal from the Early Cretaceous of Spain and its palaeogeographic implications. *Acta Palaeontol. Pol.* 48, 575-582 (2003).

35. Sweetman, S. C. A gobiconodontid (Mammalia, Eutriconodonta) from the Early Cretaceous (Barremian) Wessex Formation of the Isle of Wight, southern Britain. *Palaeontology* 49, 889-897 (2006).

36. Lovell, J. E. & Getty, R. The hair follicle, epidermis, dermis, and skin glands of the dog. *Am. J. Vet. Res.* 18, 873-885 (1957).

37. Whiteley, H. J. Giant compound hair follicles in the skin of the rabbit. *Nature* 181, 850 (1958).

38. Evans, H. E. & de Lahunta, A. *Miller´s anatomy of the dog*. 2012 (Elsevier Saunders, St. Louis, Missouri, 2012).

39. Spencer, B. & Sweet, G. The structure and development of the hairs of monotreme and marsupials. *Q. J. Microsc. Sci.* 36, 549-588 (1899).

40. Hausman, L. A. The cortical fusi of mammalian hair shafts. *Am. Nat.* 66, 461-470 (1932).

41. Rudnicka, L., et al. in *Atlas of Trichoscopy - Dermoscopy in Hair and Scalp Disease* (eds Rudnicka, L. Olszewska, M. & Rakowska, A.) 11-46 (Springer, London, Heidelberg, New York, Dordrecht, 2012).

42. Vincent, J. F. V. & Owers, P. Mechanical design of hedgehog spines and porcupine quills. *J. Zool.* 210, 55-75 (1986).

43. Montandon, S. A. et al. Two waves of anisotropic growth generate enlarged follicles in the spiny mouse. *EvoDevo* 5, 33 (2014).

44. Weibel, E. R. et al. Design of peripheral airways for efficient gas exchange. *Resp. Physio. Neurobi.* 148, 3-21 (2005).

45. Dal Sasso, C. & Signore, M. Exceptional soft tissue preservation in a theropod dinosaur from Italy. *Nature* 392, 383-387 (1998).

46. Bramble, D. M. & Jenkins, F. A. Mammalian locomotor-respiratory integration: implications for diaphragmatic and pulmonary design. *Science* 262, 235-240 (1993).

47. Campione, N. E. & Evans, C. C. A universal scaling relationship between body mass and proximal limb bone dimensions in quadrupedal terrestrial tetrapods. *BMC Biol.* 10, 60, doi:10.1186/1741-7007-10-60 (2012).

48. Foster, J. R. Preliminary body mass estimates for mammalian genera of the Morrison Formation (Upper Jurassic, North America). *PaleoBios* 28, 114-122 (2009).

49. Kirk, E. C. et al. Intrinsic hand proportions of eucharchontans and other mammals: Implications for the locomotor behavior of plesiadapiforms. *J. Hum. Evol.* 55, 278-299 (2008).

50. Stanley, W. T. et al. A. A new hero emerges: another exceptional mammalian spine and its potential adaptive significance. *Biol. Lett.* 9, 20130486 (2013).

Acknowledgements Research funds were provided by Spanish MINECO**,** Project CGL-2013-42643 P and Junta de Comunidades de Castilla-La Mancha. We thank José Luis Sañudo for finding the specimen, Mercedes Llandres and Olaf Dülfer for preparation, Dorothea Kranz for artwork, Oscar Sanisidro for life reconstruction, Georg Oleschinski for photography, Marta Furió and Andrés Valera for SEM, Kai Jäger for 3D reconstructions, and Tom McCann for improving the English. Bastian Mähler is thanked for discussion on actuo-taphonomical experiment with rat carcass.

Author contributions A.D.B. designed the Las Hoyas research project, J.M.-L., R.V., H.M.-A., and A.D.B. participated in the fieldwork, T.M., J.M.-L., R.V., H.M.-A., Z.-X.L., and A.D.B. organized and conducted the research (preparation, CT-scan, light microscopy, and SEM imaging) and analyzed data, Z.-X.L. performed phylogenetic analyses, and T.M., J.M.-L., R.V., Z.-X.L., and A.D.B. wrote the manuscript.

Figure Legends:

Fig. 1. New Early Cretaceous gobiconodontid *Spinolestes xenarthrosus*. a. skeletal reconstruction from the type specimen. b. Drawing of holotype MCCMLH30000A with skeletal element identification and outline of preserved integument. Arrow points to skin patch preserving hair

bundles, placed between dorsal vertebrae 11 and 14. Inset: Left calcaneus in dorsal view, on the transferred slab separate from the skeleton. c. Reconstruction of right hand. Numerals designate finger rays. Abbreviations: C, caudal vertebra; D, dorsal vertebra; l, left; r, right; ra, radius; S, sacral vertebra; ul, ulna.

Fig. 2. Dentition and xenarthrous vertebrae of *Spinolestes*. a. Reconstruction of dentition with deciduous molariforms (grey shading). b. SEM image of penultimate (m3) and ultimate (m4) right lower molariforms in lingual view. c. SEM image of anterior portion of skull and mandibles with dentition. d. SEM images (stereo-pair) of right lower mandible and right upper maxilla with molariforms. Abbreviations: C/c, upper/lower canine; I/i, incisor; M/m, molariform; P/p, premolar; D/d, deciduous tooth; R/r, replacing tooth. e. SEM images (stereo-pair) of dorsal vertebrae 11 to 19 in lateral aspect with ribs. f. Close-up of dorsal vertebrae 15 to 18 with xenarthrous articulations, SEM images (stereo-pair). g. Drawing of dorsal vertebrae 15 to 18 with accessorial (xenarthrous) lateral articulations. Abbreviations: az, anterior zygapophysis; alz, anterior lateral zygapophysis; pz, posterior zygapophysis; plz, posterior lateral zygapophysis.

Fig. 3. Phylogenetic relationships of *Spinolestes* and patterns of mammalian integumentary structure in early mammalian evolution. a. Position of *Spinolestes* within Eutriconodonta (Bremer index/bootstrap values on the key clades of this study). b. Evolution of mammalian integumentary structures (simplified tree). Datasets and full analyses presented in Supplementary Information.

Fig. 4. New gobiconodontid *Spinolestes xenarthrosus*, holotype counter slab (MCCMLH30000B) and integumentary structures. a. Holotype counter slab with its half skeleton on original rock matrix. b. Guard hairs of dense fur (mane) in the cervical region (AT, atlas). c. Hairs and keratinous dermal scutes (SC) from portion of integument placed between dorsal vertebrae 11 and 14. d. Arrangement of compound hair follicles (inset) including hair bulbs (HB), primary hairs (PH) and secondary hairs (SH). e. Area with protospines, dermal scutes (SC), and isolated tubules (inset). f. Protospines (PS) and isolated tubules (T) under translucent light. g. SEM image of a primary hair shaft's longitudinal section displaying inner structure with cortex (C) and medulla of discontinuous type (M). h. Oval keratinous dermal scute (SC) dorsally of left ischium (ISC-L) with tubules and the homogeneous matrix. i. SEM image of compound follicle (FO) with primary (thicker) hair of mosaic cuticular pattern and secondary (thinner) hairs with coronary (annulus) cuticular pattern. j. Underfur hairs with

annular cuticular pattern in the abdominal region under translucent light. c-f and j from transferred slab MCCMLH30000A.

Extended Data Figures Legends:

Ext. Data Fig. 1. New gobiconodontid *Spinolestes xenarthrosus*, holotype transferred slab MCCMLH30000A. Skull exposed in ventral aspect. Inset: Left calcaneus in dorsal view on the same slab somewhat apart from the skeleton. Arrow points to skin patch preserving hair bundles between dorsal vertebrae 11 and 14.

Ext. Data Fig. 2. Skin structures of *Spinolestes*. a. SEM image of skin surface showing compound hair follicles (FO), epidermal cells (keratinocytes), and pores (P). b. Schematic drawings of scale-like skin folds (SCF) with compound hair follicles (FO) of the dog with primary (PH) and secondary hairs (SH) of three ontogenetic stages (redrawn from ref. 36). c. Skin surface of *Spinolestes* with scale-like wrinkles. d. Schematic diagram of scale-like wrinkled skin folds with hair follicles of a dog (redrawn ref. 34). e. SEM image of epidermal cells (keratinocytes) of a hair follicle. f. SEM images of skin surface with polygonal epidermal cells (keratinocytes) and pores. g. Detail of the keratinocytes.

Ext. Data Fig. 3. SEM images and interpretative line drawings of cuticular scale patterns of primary (largest, a and b) and secondary hairs (b and c).

Ext. Data Fig. 4. Hair structures of *Spinolestes*. a, c, and d. Patch of skin located between dorsal vertebrae 11 and 14 (arrow in fig. 1 and 4) at the slab MCCMLH30000A under translucent light. b. SEM image of an orifice of a compound follicle with primary hair and three broken secondary hairs. Abbreviations: HB, hair bulb; PH, primary hair; SH, secondary hair.

Ext. Data Fig. 5. a. Details of hair cortex. a. SEM image of a fraying hair of *Spinolestes* showing longitudinally fused tubular cells. b. Schematic diagram of human hair bulb (B) with cuticular scales (CU) and fusi (F) at the hair shaft (HS). c. Schematic diagram of a human head hair with fusiform cortical cells (FCC) and fusi. b and c redrawn from ref. 38.

Ext. Data Fig. 6. External pinna of *Spinolestes* (a, b) in comparison with pinna and scalp of decaying rat (*Rattus norvegicus*). a. On transferred slab MCCMLH30000A. b. On counter slab MCCMLH30000B on original limestone rock matrix. c. Head of decaying rat after 274 days in water at room temperature. The skull is detached from the scalp and has fallen to the bottom. Scalp and right pinna are still intact and connected to the floating carcass. D. Detail of c with well-preserved right pinna in original position at the scalp. The mandible is displaced and loosely hanging down from the skin.

Ext. Data Fig. 7. Keratinous dermal scutes (SC) of *Spinolestes*. a. Oval dermal scutes dorsally of dorsal vertebra 20. b. Oval dermal scutes dorsally of left ischium (ISC-L). c. Oval dermal scute from dorsal region with tubules (T) merging to homogeneous keratinous matrix.

Ext. Data Fig. 8. Visceral cavities of *Spinolestes* with internal organs. a. Detail of the visceral cavities of MCCMLH30000B with separation of the anterior thoracic cavity (TC) containing the lungs (LU) and the posterior abdominal cavity (AC) containing the liver (LI). Dashed line represents the diaphragm. b. Lung tissue in the anterior part of the thoracic cavity. c. Peripheral conducting and acinar airways of the lungs with typical dichotomous structure of the bronchial tree. d. Peripheral conducting and acinar airways of the lungs from transferred slab MCCMLH30000A under translucent light. e and f. Details of the peripheral conducting airway dichotomies (DI) and acinar structures (ACI) of the lungs.

Ext. Data Fig. 9. Life reconstruction of *Spinolestes xenarthrosus*.

Methods Upon discovery, the rock containing the specimen was split into two slabs each containing original bone, fossilized soft tissues, and natural molds of bones. One slab (MCCMLH30000A) was transferred to a matrix of epoxy resin to expose undisturbed bone surface hidden in the rock and to obtain casts of the natural molds of bone impressions. After embedding in epoxy resin, the limestone matrix was removed by a formic acid bath that dissolved the calcium carbonate but not the hydroxyapatite of bone and the phosphatized soft tissue. The transparent artificial plastic matrix allows examination of integument structures under translucent light. The other slab (MCCMLH30000B) was left untouched in the limestone matrix to keep its original embedding situation.

The transferred slab and the non-transferred slab were scanned on a v|tome|x s µCT-scanner at 240 kV (GE Electronics Phoenix|x-ray), 864 slices at a voxel size of 107.73 µm. Resolution was electronically enhanced (voxel size 53.86 µm) by Datos|x-reconstruction software (Version 1.5.0., GE Sensing Inspection Technologies). Reconstructions (Videos S1, S2) by Avizo (Version 8.0, Visualization Science Group).

Two phylogenetic analyses were performed using PAUP (4.0b10) to estimate the placement of *Spinolestes* among eutriconodont mammals and their immediate outgroups, and among major cynodont-mammal clades. The analysis of eutriconodonts was based on a dataset augmented from refs. 18, 31, 32. The matrix has 29 taxa (20 eutriconodonts plus nine outgroups) and 87 parsimony-informative characters. In the search of this matrix, all characters have equal weight, six multi-state

characters are ordered, and remaining characters un-ordered. The branch-and-bound, which guarantees the shortest tree, has yielded a single most parsimonious tree (tree-length = 249; Consistency Index [CI] = 0.446; Retention Index [RI] = 0.755), as presented in Fig. 3a. Nodal strengths of key clades are also assessed by bootstrap values (based on a 50% majority rule consensus from 1000 duplicates of bootstrap searches), and by Bremer index. Details in Supplementary Information.

Phylogenetic analysis of *Spinolestes* among major clades of cynodonts and mammals was based on a dataset expanded and modified from that of ref. 6. The data matrix has 112 taxa (including eight eutriconodonts), 490 characters (all parsimony-informative). The phylogenies were estimated by 1000 replicates of heuristic search with tree-bisection-reconnection (TBR) branch-swapping algorithm. All multi-state characters are unordered; all characters have equal weight. The search yielded 172 equally parsimony trees (EPT) (each EPT has a tree length of 2386 steps). Strict consensus tree of the 183 EPTs is presented in Supplementary Information and a simplified tree is presented in Fig. 3b.

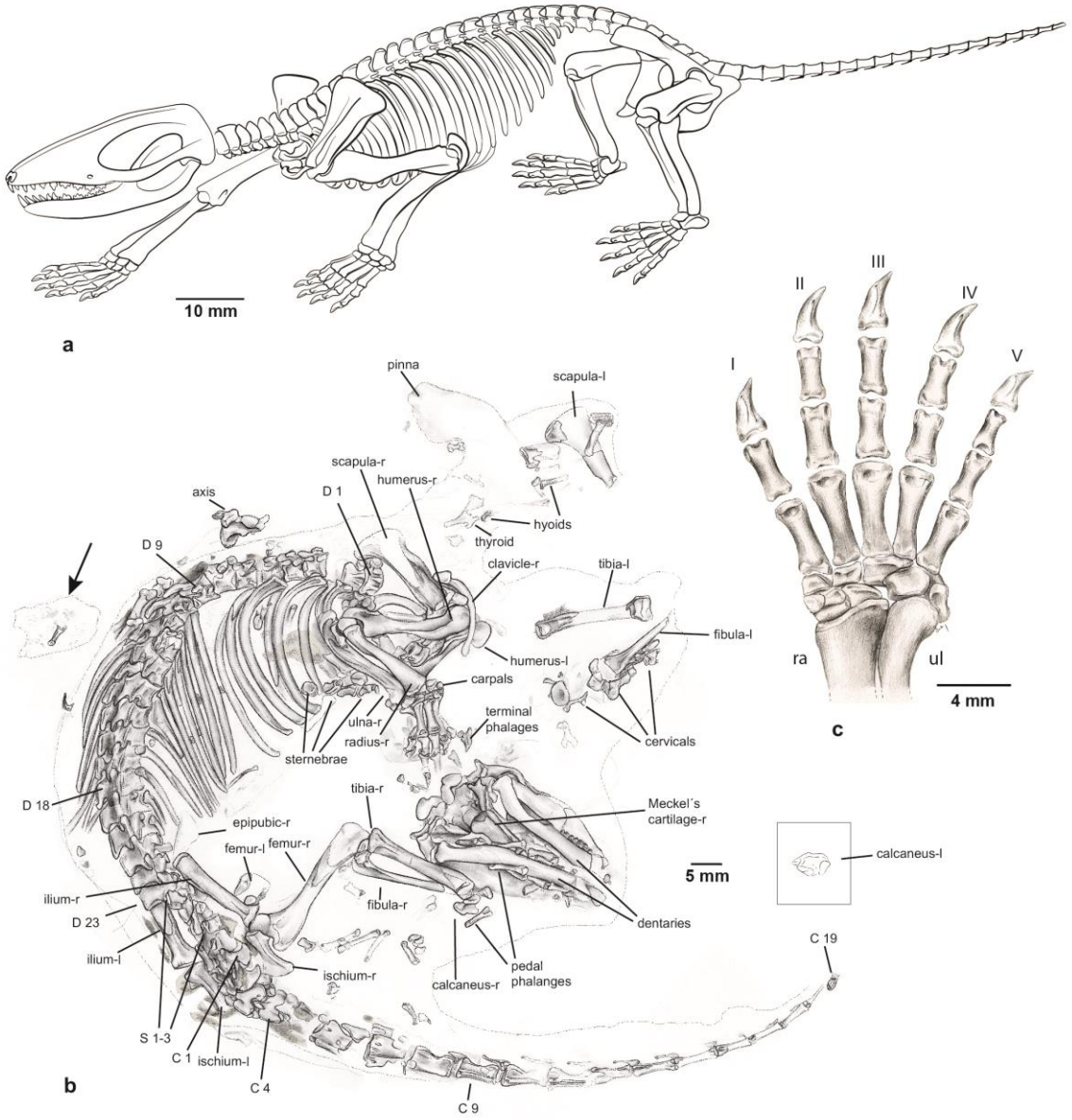

Fig. 1 New Early Cretaceous gobiconodontid Spinolestes xenarthrosus

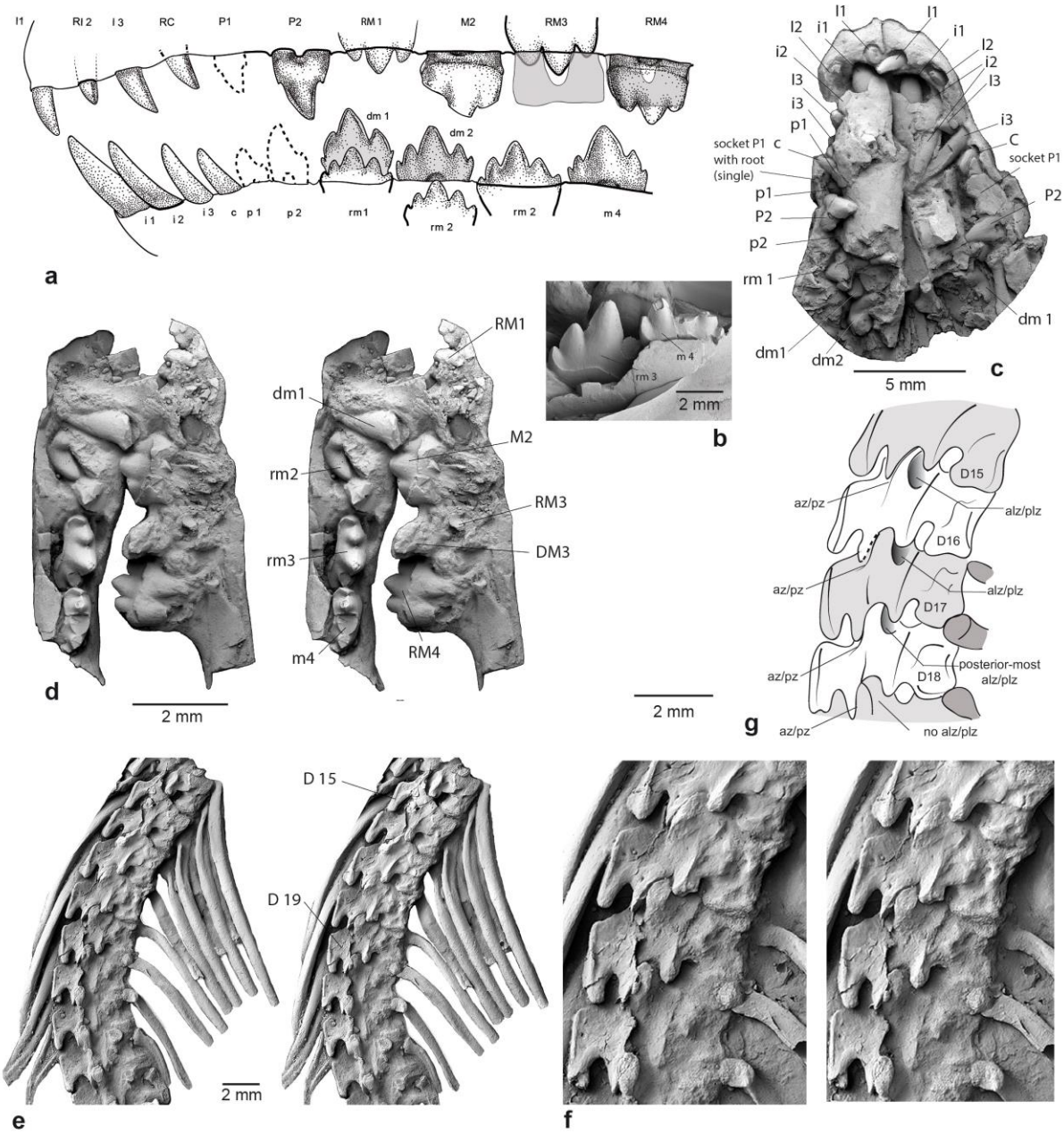

Fig. 2. Dentition and xenarthrous vertebrae of Spinolestes.

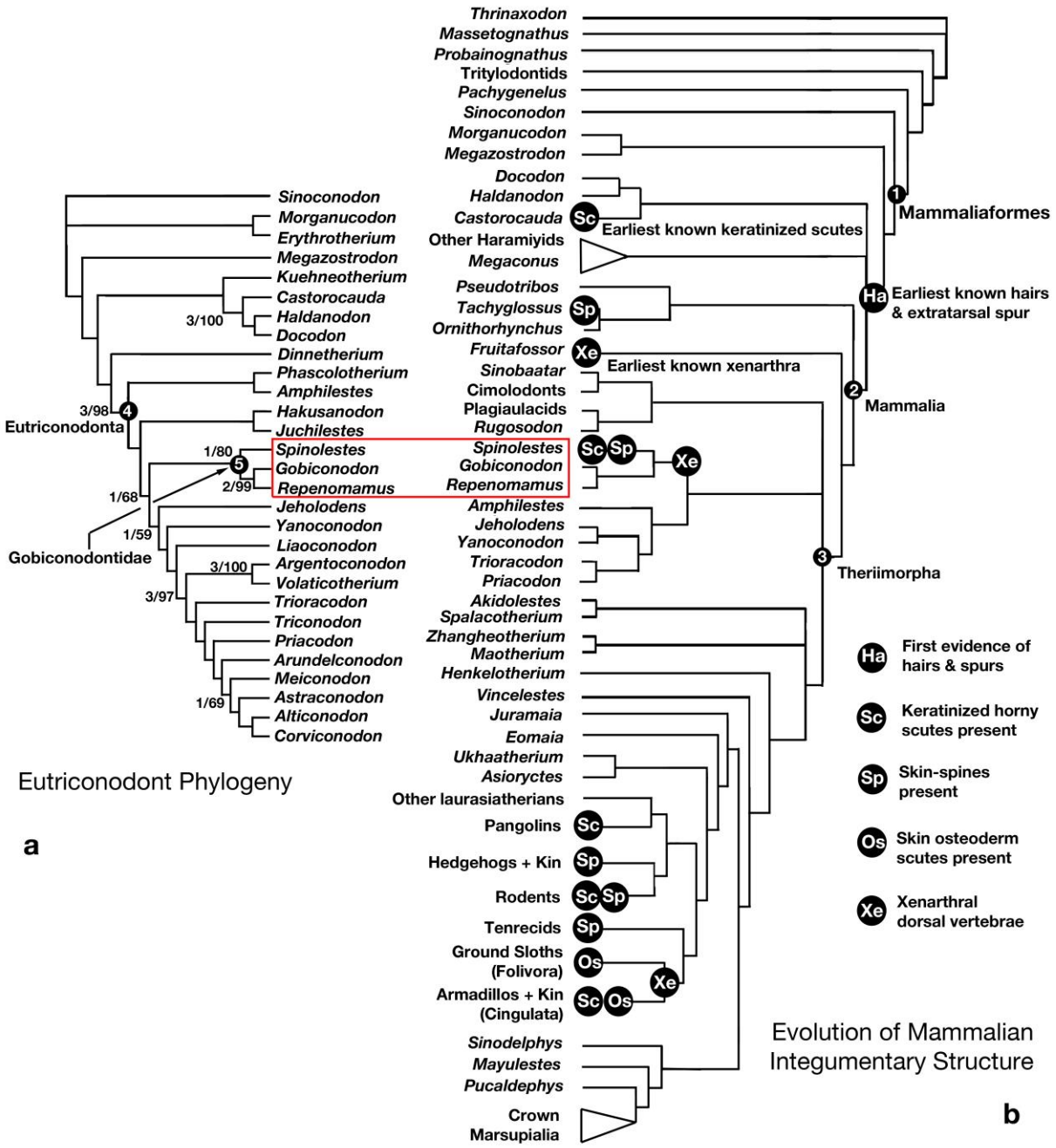

Figure 3 Phylogenetic relationships of Spinolestes and patterns of mammalian integumentary structures in Early Mammalian Evolution (10 June 2015 revision)

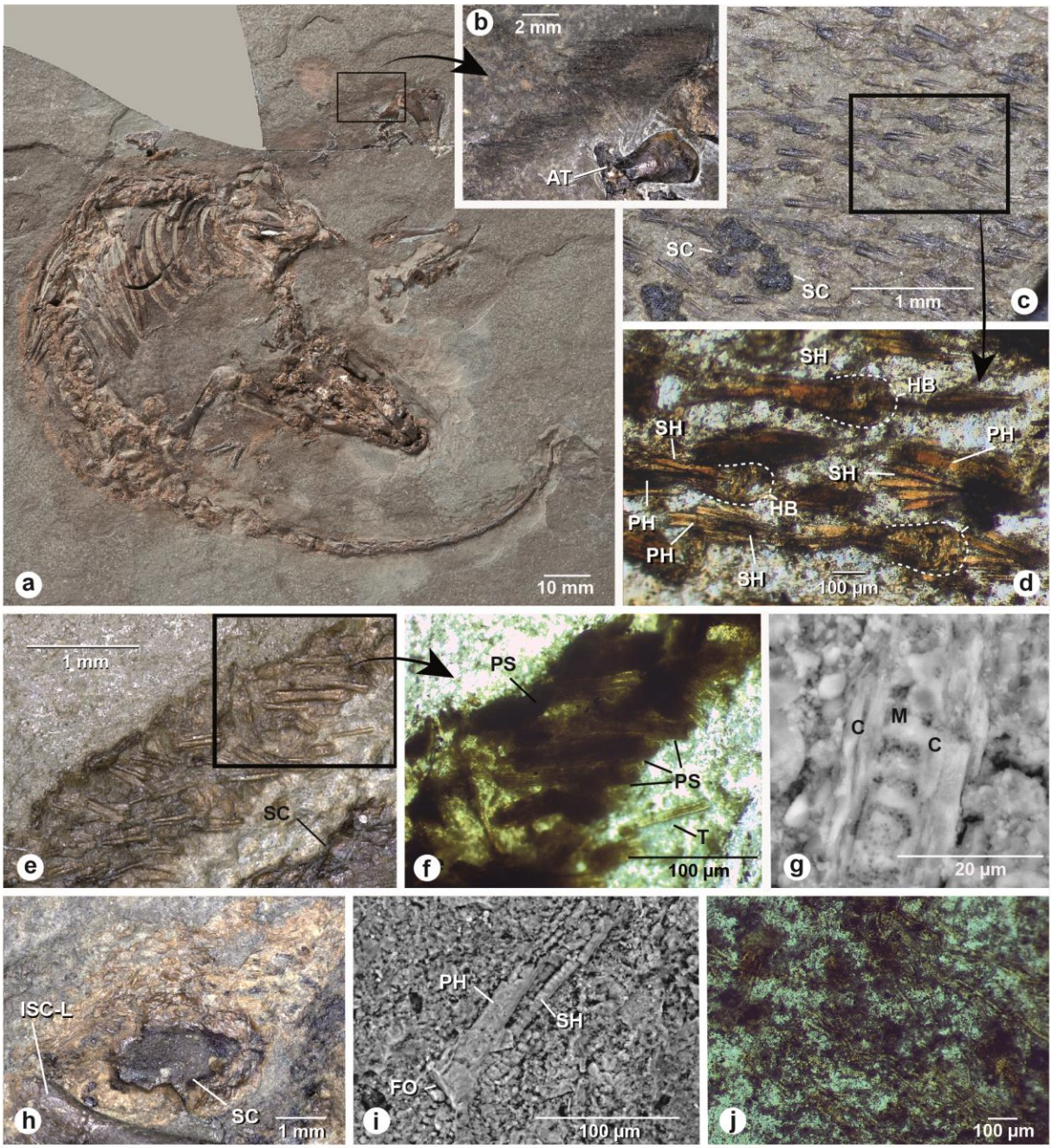

Fig.5. New gobiconodonttid Spinolestes xenarthrosus, holotype counter slab (MCCMLH30000B) and intergumentary structures

Fig. 4. New gobiconodontid *Spinolestes xenarthrosus*, holotype counter slab (MCCMLH30000B) and integumentary structures